Marine Geology, 108 (1992): 259–274
Elsevier Science Publishers B.V., Amsterdam

The longshore flow component in low-energy rip channels: The Mediterranean, Israel

D. Bowman[a], H. Birkenfeld[a] and D. S. Rosen[b]

[a]*Ben-Gurion University of the Negev, Beer-Sheva, 84105, Israel*
[b]*National Institute of Oceanography, Israel Oceanographic and Limnological Research, Haifa 31080, Israel*

(Received April 22, 1992; accepted July 23, 1992)

ABSTRACT

Bowman, D., Birkenfeld, H. and Rosen, D. S., 1992. The longshore flow component in low-energy rip channels: The Mediterranean, Israel. *Mar. Geol.*, 108: 259–274.

We examined in the field the near-bed longshore (v) flow component in rip channels at the Herzliyya beach, Israel, on the Southeastern Mediterranean. Field experiments, conducted under relatively calm wave conditions (T_{sig} = 3–6 s, H_{sig} = 0.3–1.1 m) included current and wave monitoring and morphological mapping. Time series of instantaneous and smoothed shore-parallel current velocities and of the orbital components, were analysed, including statistical and spectral processing.

The peak instantaneous velocities of waves and currents combined were in excess of the threshold motion of the local sand, taken as 0.3 m/s. Some velocities even exceeded the threshold for sheet flow transport ~0.9 m/s. The feeder and the neck demonstrated the highest longshore flow components, whereas the rip head, typically showed the lowest longshore velocities. The unsteadiness of the net longshore current was very high. Feeders typically showed a mean unidirectional longshore current. However, directional fluctuations gradually increased towards the rip head.

The data suggest a clear spectral structure; most energy (46–67%) was in the gravity range with 13–35% subharmonic and minor (13–16%) in the infragravity band. Systematic cross-shore spatial trends of the energy spectra components were linked to bar morphology and to exposure to incident waves.

Introduction

The first detailed nearshore circulation measurements were reported by Shepard and Inman (1950). The dynamics of rip currents have been further examined by Arthur (1962), Draper and Dobson (1965), Bowen (1969), Bowen and Inman (1969), Cook (1970), Sonu (1972) and by Tam (1973).

Additional data on the rip environment is included in the studies of Clifton (1976), Davidson-Arnott and Greenwood (1974, 1976), Greenwood and Davidson-Arnott (1979), Lenhart (1979), Greenwood and Hale (1980), Wright (1982), Basco (1983), Short (1985) and Bowman et al. (1988a,b). These studies examined various flow characteristics along rips, including vertical velocity profiles, velocity time asymmetry, pulsation, formation of offshore dipping structures and long-term behavior.

Despite theoretical work (Longuet-Higgins and Stewart, 1964; Longuet-Higgins, 1970; Noda, 1974; Sasaki and Horikawa, 1975; Birkemeier and Dalrymple, 1975; Komar, 1976; Wu and Liu, 1985) there have been, however, relative few detailed small-scale studies documenting the longshore current across non-planiform, complex barred bathymetry. Allender and Ditmars (1981) reported unexpected uniform longshore current velocity profiles up to 1.8 m/s during storms across an entire surf zone, despite the barred topography. The vertical variability of longshore currents in a barred surf zone was found by Greenwood and Sherman (1983) not to deviate > 1% of the depth averaged velocity. Keeley and Bowen (1977)

Correspondence to: D. Bowman, Ben-Gurion University of the Negev, Department of Geography and Environmental Development, P.O. Box 653, Beer-Sheva, 84105, Israel.

0025-3227/92/$05.00

showed rip current sites to have a diminished longshore flow. Sasaki and Horikawa (1978) reported rip currents at the convergence point of two opposed flow directions to be "zero crossing" sites for the longshore current direction. However, even without reversal of directions, the location of rip currents marks a sharp reduction in the strength of the longshore current (Huntley et al., 1988).

This paper is based on detailed field experiments carried out on beaches of longshore rythmic transverse bars and rips. We focus on the near-bottom horizontal longshore flow component in low-energy rip channels. The aim is to unravel the longshore current in the accretional rip type (Short, 1985), from the shore-parallel feeder through the transverse or oblique neck segment, up to the rip head.

Study area

The study area is located in the Southeastern Mediterranean, within the litoral cell of the Nile (Fig. 1). An eastnorthward net longshore current domains the cell from the Nile delta up to Haifa (Neev and Emery, 1967; Goldsmith and Golik, 1980; Carmel et al., 1984). The study site of Herzliyya is located north to Tel-Aviv. The beach is oriented N13°E with a uniform foreshore slope of 0.6°–1.3° and backed by a coastal eolianite cliff. The study area has a narrow surf zone with breakers on the inner bar and a microtidal range averaging less than 50 cm. The prevailing wave characteristics during the study period were H_{sig} = 0.3–1.1 m, H_{max} = 0.4–1.9 m and T_{sig} = 3–6 s, with a W–WNW incident wave direction all of which are typical of summer storms to fairweather conditions. The beach is composed of medium-sized sand. The gross average size is 1.87ϕ (272 μm) ranging 1.5ϕ–2.2ϕ (217–354 μm) and sorting is good $\sigma\phi$ = 0.47.

We applied the surf scaling parameter for defining the morphodynamic beach state (Guza and

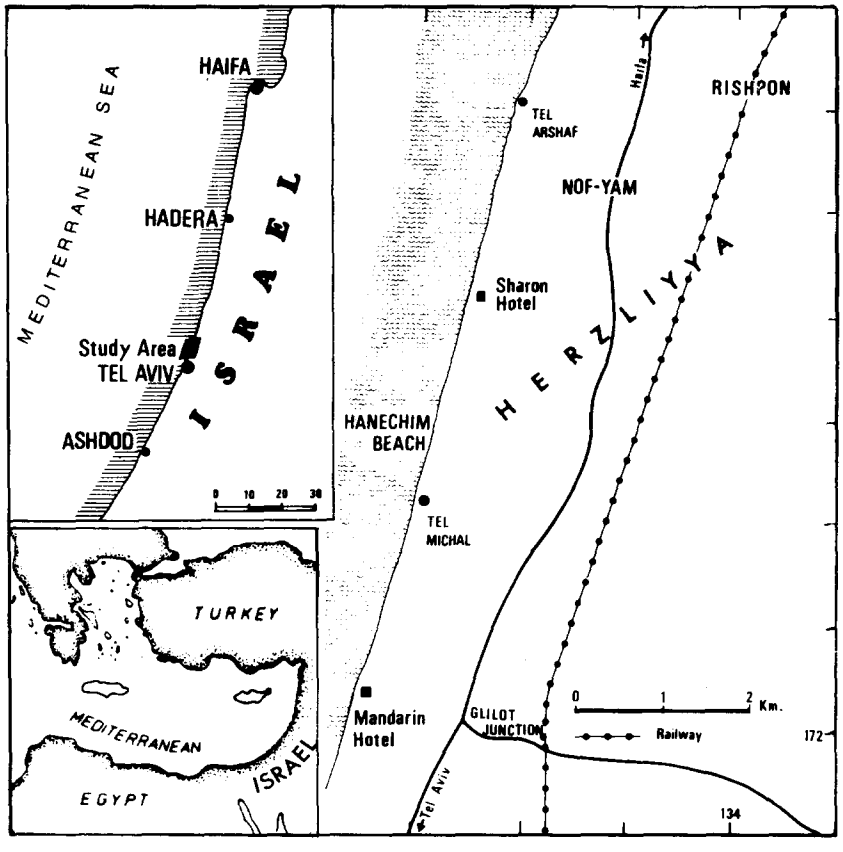

Fig. 1. Location maps.

Inman, 1975) $\varepsilon = \alpha \cdot \omega^2/g \cdot \tan^2 \beta$, where α = incident wave amplitude near the point of wave breaking, $\omega = 2\Pi/T$, T = wave period, g = acceleration of gravity and β = inshore–foreshore slope. The modal beach state and the energy environmental characteristics have been also defined by the dimensionless beach state parameter (Dean, 1973) $\Omega = H_b/TW_s$, where H_b is the breaker height, T is the peak breaker period and W_s is the fall velocity of the beach sediment.

The rip embayments in the study area are characterized by high to moderate ε values in the range 6–55, indicating a dissipative to transitional beach state. The Ω values ranged 3–4, similarly indicating an intermediate beach state. The rips alternate within megacusp embayments between welded, transverse and skewed rhythmic bars, forming circulation cells which are typical of beaches in the intermediate state (Wright, 1982).

Methods

Field data

Field data were collected twice monthly from March to October. Each experiment started with a flight over the study area for observation and photography. Two bidirectional electromagnetic current meters (type M-512, Marsh-McBirney) with time constants of 0.5 s were shifted from one recording station to the next in the surf zone, along rip channels, resulting in a total of 63 monitored sites. The calibration uncertainty associated with these flowmeters is in the 5–10% range

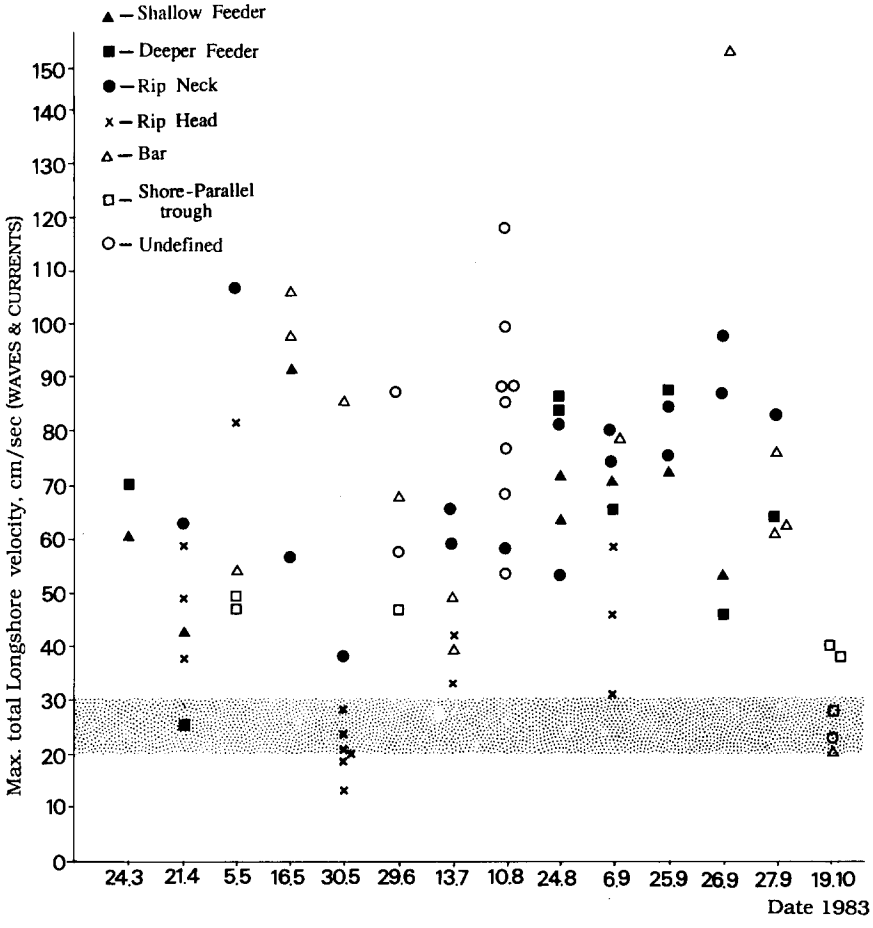

Fig. 2. Peak instantaneous longshore velocities of waves and currents demonstrating a major exceedance of the threshold velocity for sand motion (0.2–0.3 m/s) and some exceedance of the threshold criteria for sheet flow (0.9 m/s).

(Cunningham et al., 1979; Guza and Thornton, 1980; Basco, 1982). The near-bottom currents were recorded with the sensing elements mounted at $Z = 36$ cm above the bed.

In order to record the horizontal longshore current, the current meters were installed at a fixed N13°E orientation which had been determined by compass and maintained by pins fixed into the

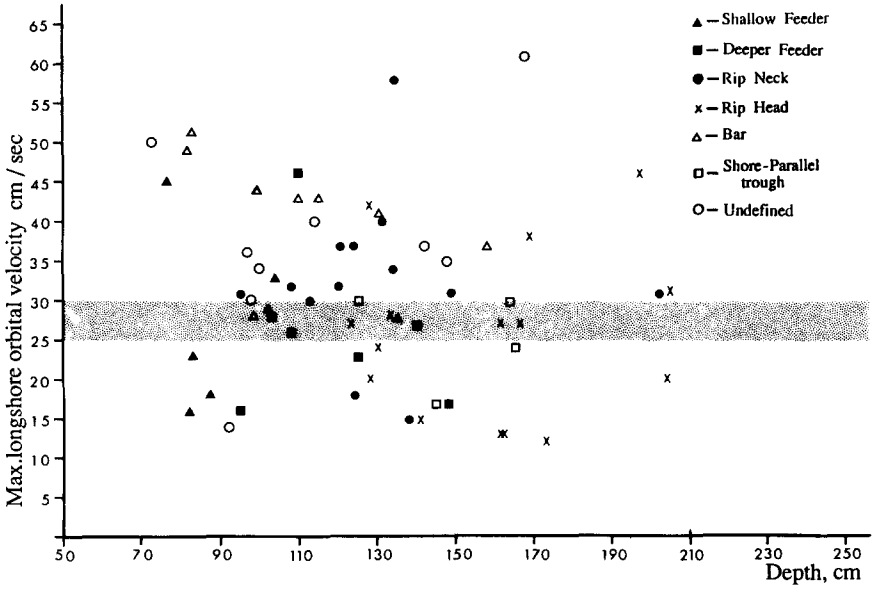

Fig. 3. Peak instantaneous longshore orbital velocities. Note some exceedance of the threshold for sand motion (0.2–0.3 m/s), but none of the threshold velocities for sheet flow transport.

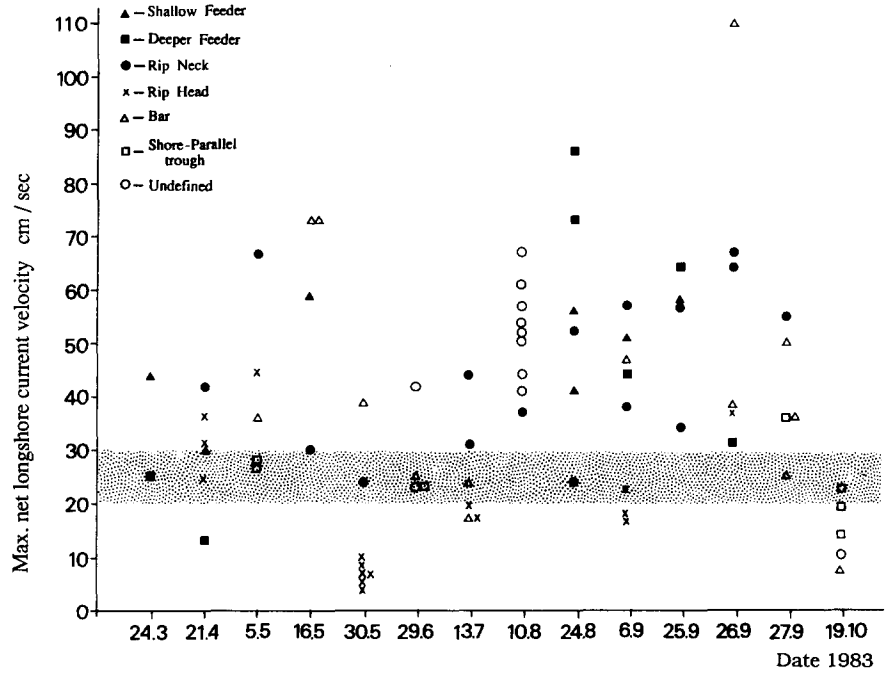

Fig. 4. Maximum net longshore current velocities demonstrating capacity of sand activation (>0.3 m/s).

seabed. The sensors were hardwired to the beach and logged on a multichannel A/d magnetic tape cassette data-logger and were simultaneously chart-recorded. Data were scanned by a multiplexer at the rate of 1.875 Hz/channel. Ten tape malrecorded stations were digitized from the paper chart records and logged on a magnetic tape in the same format. Bathymetric data were obtained by level and staff along survey lines which extended to the limit of the wading depth. Time series of significant wave heights and periods were determined at 3 h intervals by offshore Datawell wave riders, monitoring at Hadera, 33 km north of the study site and at Ashdod, 40 km south of Herzliyya. The applicability of the Ashdod and Hadera wave data for the entire Israel coast up to Haifa Bay had previously been affirmed by Migniot (1974), Rosen and Vajda (1979), Goldsmith and Golik (1980) and by Rosen and Kit (1981).

Data processing

The time series of the longshore current (v) component which form the primary data base, were processed in order to define their characteristic flow signatures. Each recording was cut to 2048 data points, representing 1024 s of record length, and was read by a cassette reader connected to a microcomputer system. High-frequency oscillatory velocities were removed by the "running average"

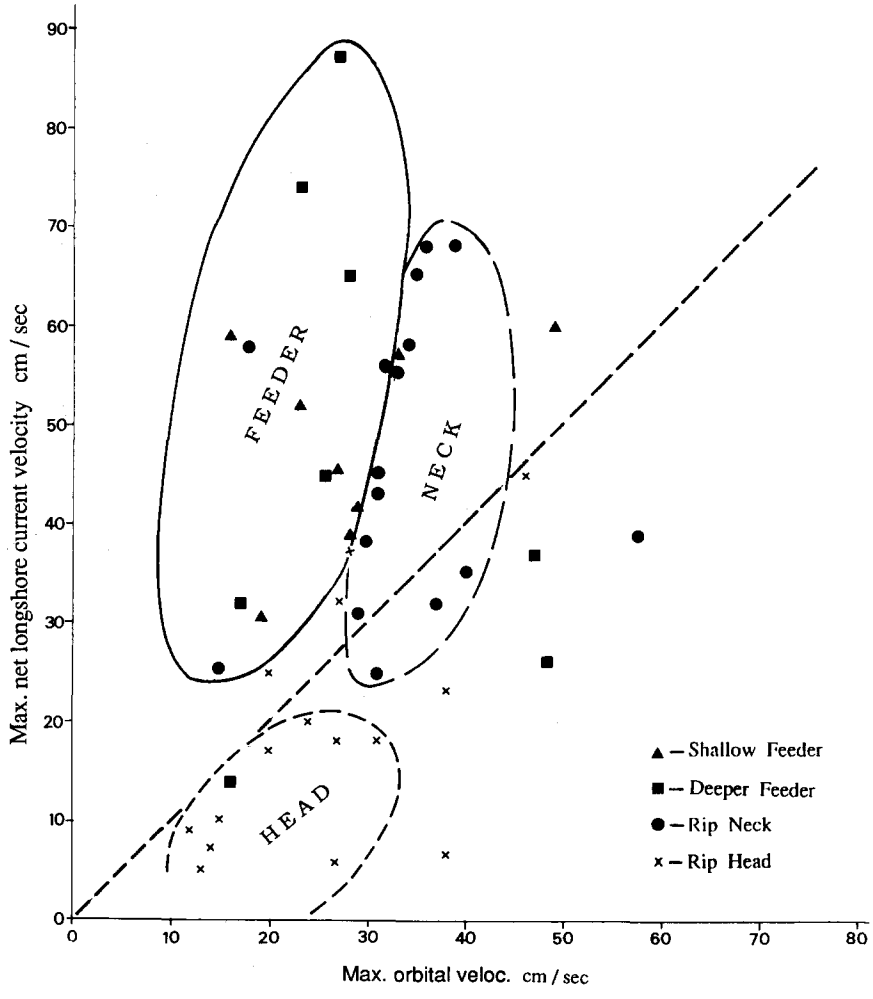

Fig. 5. Separation between the velocity fields of the head, neck and feeder in the rip system, based on the maximum orbital velocity related to the maximum net longshore current.

smoothing method. A cosine window, 18.5 s wide, was applied to remove shorter than subharmonic orbital wave motions. The resulting signals, after filtration, were regarded as being generated mainly by tidal, longshore, rip and general circulation currents. Processing included decomposition of the time series into the oscillatory wave-induced orbital motion and the net direct current. Flow asymmetry was analysed with respect to both magnitude and duration and was further identified by comparing the cumulative offshore- and onshore-directed discharges. The time-averaged current vector and velocity and the direction distribution of each record were also computed (Kit et al., 1985).

Energy spectra of the total longshore current, including current and waves, were computed by means of the fast Fourier transform. The computation included the peak period for each spectra distribution, with the low-frequency cut at 1/180 s. The frequency range was divided into three domains, as follows: (1) A domain attributed to infragravity waves, corresponding to the frequency range $< 1/(5T_p)$ where T_p is the spectral peak period. (2) A frequency range attributed to subharmonic edge waves corresponding to the frequency range $1/(1.5T_p)$–$1/(5T_p)$, and (3) A frequency range corresponding to periods of gravity waves in the 2.5–15 s range.

Daily bathymetric maps were prepared by manual interpolation of the data and with the aid of overflight observations and field notes. Each recording station was environmentally defined according to the characteristics of its location. The following inshore subenvironments were obtained:

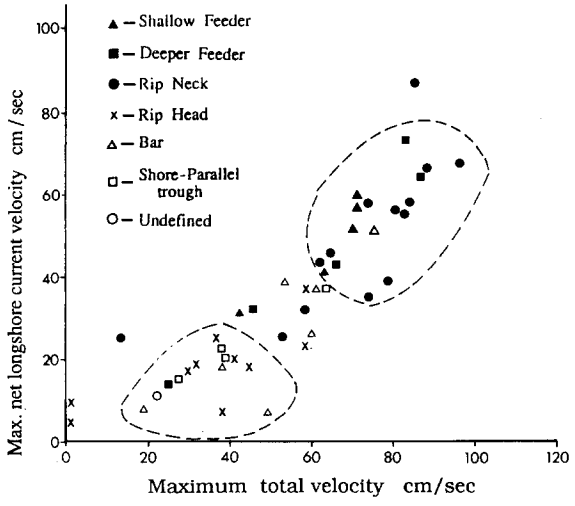

Fig. 6. Maximum total longshore velocity (waves and currents) at various subenvironments in the rip system related to the maximum net longshore current. Note that the field of the neck and the feeders is separated from that of the rip head.

oblique and parallel bars, shore-parallel channels, the uppermost shallow feeder segment, the wider and deeper segment of the feeder, the rip neck, the rip head off the oblique-transverse bars and morphologically undefined offshore sloping surfaces in the inshore.

The shifting of flowmeters during each field experiment from one recording site to the next could have resulted in superposition of hourly wave climate changes on the spatial environmental characteristics, i.e., substitution of space by time. However, the daily range of the significant wave height was low (8–24 cm) and unrelated to the spatial trends, which suggests that the hourly wave

TABLE I

Mean percentage of the longshore current energy frequency bands at different sites in the rip system. T_p indicates peak period

Spectra bands	$>5T_p$	1.5–$5T_p$	2.5 s–1.5 T_p	
Energetic domain	A infragravity	B subharmonic	C incident	Sample (n)
Environment				
Shallow feeder	16.35	35.10	48.38	8
Deep feeder	16.37	27.01	56.50	8
Rip neck	17.47	19.64	62.76	15
Rip head	13.70	19.16	66.96	15
Bar	11.89	20.45	67.52	14

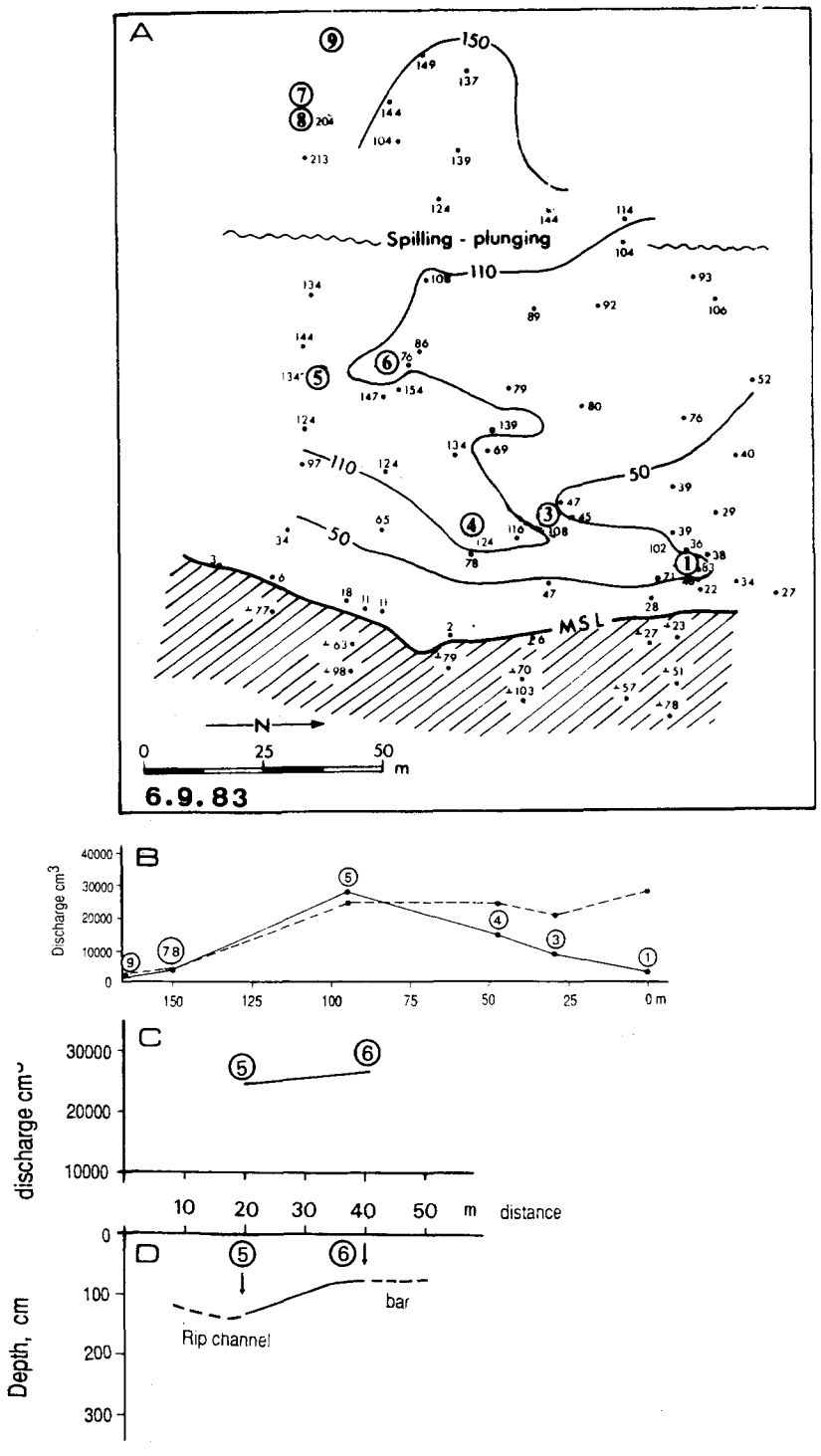

Fig. 7. Bathymetry and flow characteristics across oblique rip channels determined on September 6, 1983. (A) Bathymetry, recording sites are encircled, depth in centimeters. (B) Net longshore velocities (broken line) compared to offshore rip velocities (unbroken line) shown as discharge. Note decrease of the net longshore velocity towards the offshore. (C) Change of longshore velocities when current enters a rip channel after crossing an oblique bar. (D) Bathymetric section.

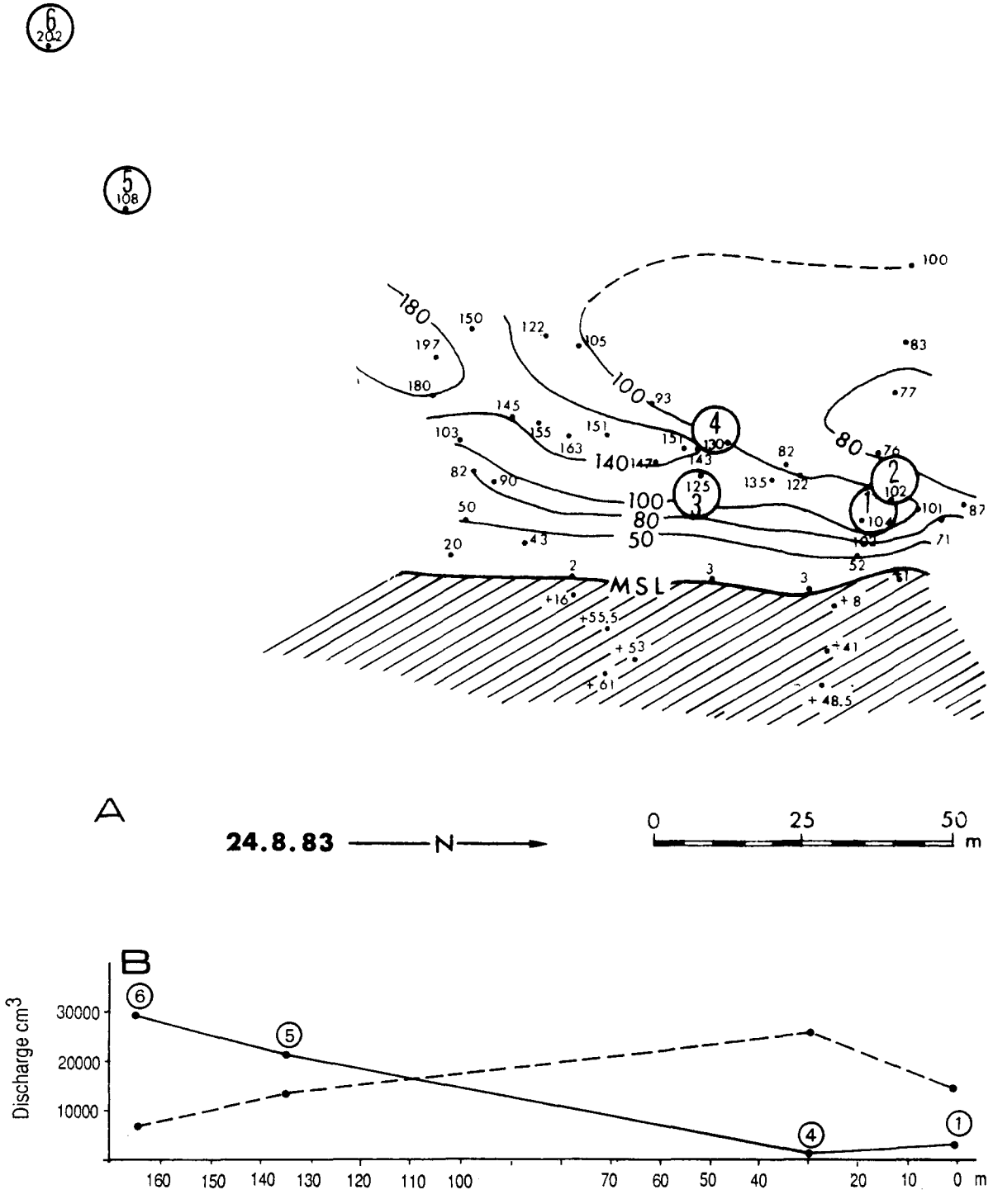

Fig. 8. Bathymetry and flow characteristics across oblique rip channels determined on August 24, 1983. (A) Bathymetry, recording sites are encircled, depth in centimeters. (B) Net longshore velocities (broken line) compared to offshore rip velocities (unbroken line) shown as discharge. Note decrease of the net longshore velocity towards the offshore.

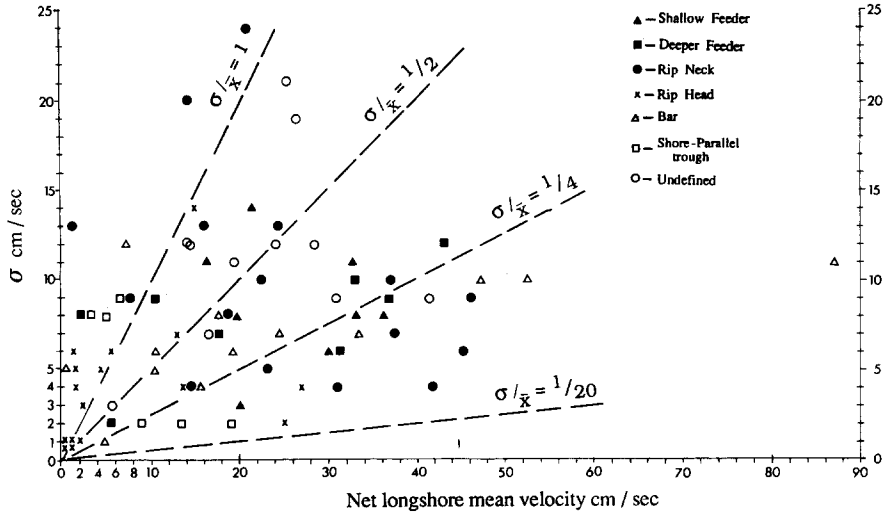

Fig. 9. Unsteadiness of the net longshore current shown as RMS related to the mean net longshore velocity. Many recordings demonstrate very high fluctuations, with $\sigma/\bar{x}$ over 0.5.

fluctuation factor could be ignored and the current records regarded as time-independent.

Results

Shearing capacity

The competence of the waves and currents, i.e., the orbital wave motion combined with the net longshore current, to activate sand is examined in Fig. 2. The data demonstrate that except at the calmest periods of May and October, the peak instantaneous velocities are in excess of the threshold motion for the local sand, taken as 0.3 m/s. Taking Dingler and Inman's (1977) threshold criteria for sheet flow transport ~0.9 m/s, the peak instantaneous total longshore velocities show some exceedance of this criterion. Peak orbital instantaneous velocities (Fig. 3) also often exceed the threshold motion for the beach sand, however, the minimum threshold criteria for sheet sand transport ~0.6 m/s (Allen, 1985) is not exceeded. The less powerful net longshore current (Fig. 4) is in many cases also effective in initiating sediment motion.

Velocity characteristics

By comparing the longshore orbital component to the net residual longshore flow (Fig. 5) and the total longshore velocity to the net longshore velocity component at different sites along the rip channel (Fig. 6), flow characteristics, at the various subenvironments, stand out clearly. The feeder and the neck demonstrate the highest net longshore, orbital and total longshore velocities. The rip head composes a unique flow environment, typified by the lowest longshore velocities. A clear gradual change along rip channels is thus often discerned (Figs. 7 and 8).

The unsteadiness of the net longshore current is very high with many recordings ranging over $\sigma/\bar{x} > 0.5$ (Fig. 9). No subenvironment, however, demonstrated any typical level of velocity variance except the rip head, where the very low-velocity longshore currents show the highest instability $\sigma/\bar{x} > 1.0$ and the onshore-offshore flow becomes dominant. At convering feeders of shore-normal rip systems, the longshore velocity fluctuations above the mean, shown as standard deviations, are smaller than those of the onshore/offshore flow.

Meadows (1977) appreciated the unsteadiness of longshore currents and showed in the surf zone variations in excess of 150% of the mean to occur over 3–8 s. Considerable unsteadiness with time, reaching the range of 100–150% of the mean within one wave period, has also been reported by Inman and Quinn (1952). Even on relatively straight beaches considerable time variations have

been recorded (Guza and Thornton, 1978). This wide magnitude range of oscillatory components is too large to be accounted for by fluctuations of wave-induced horizontal particle velocities, but can be expected from the non-uniform sea surface elevations alongshore and from fluctuating breaking waves, as well as from the interactive phenomena driven by the surf beat.

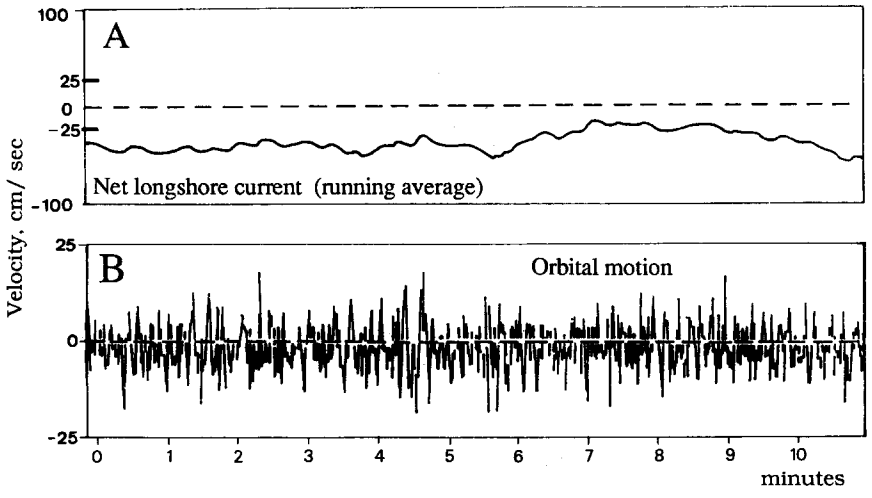

Fig. 10. Typical longshore current time series recordings comparing the instantaneous orbital motions to the smoothed net longshore current at a well-protected feeder. For location see Fig. 7. Positive values indicate northward direction. Note orbital velocity (B) is significantly lower compared to the net longshore unidirectional current (A), (station 4, date 6/9/83, water depth = 1.24 m, H_{sig} = 0.45 m).

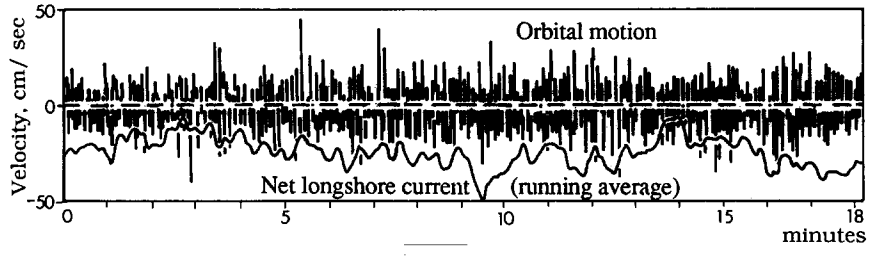

Fig. 11. Typical longshore current time series recordings comparing the instantaneous orbital motions to the smoothed net longshore current at the rip neck exposed to the incident orbital motion. For location see Fig. 7. Positive values indicate northward direction. Note stronger orbital motions and the net longshore unidirectional currents. A few instantaneous orbital peaks are beyond threshold velocity for sand entrainment (0.3 m/s), (station 6, date 6/9/83, water depths 1.76 m H_{sig} = 0.45 m).

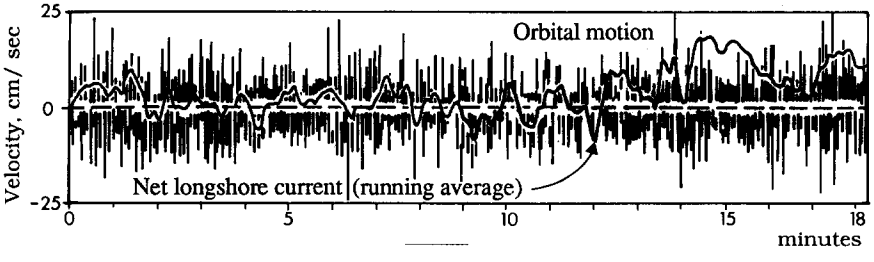

Fig. 12. Typical longshore current time series recordings comparing the instantaneous orbital motions to the smoothed net longshore current at the rip head in a transverse bar pattern. For location see Fig. 7. Positive values indicate northward direction. Note dominance of the orbital instantaneous motions over the net longshore current and fluctuating directions. (station 8, date 6/9/83, water depths 2.34 m, H_{sig} = 0.45 m).

Unidirectionality

By unidirectionality we mean an extreme directional skewness, i.e., a continuous flow, in one preferred direction, without reversals over more than 95% of a recording period of 17 min. Unidirectionality was quantified both by time and by discharge. The data indicate that most of the recordings — 56% by time and 67% by discharge — proved unidirectional. Unidirectionality is almost perfect along rip feeders, whether shore parallel or oblique (Fig. 10). Directional fluctuations increase at the rip neck (Fig. 11), whereas the rip head is the least persistent in flow direction

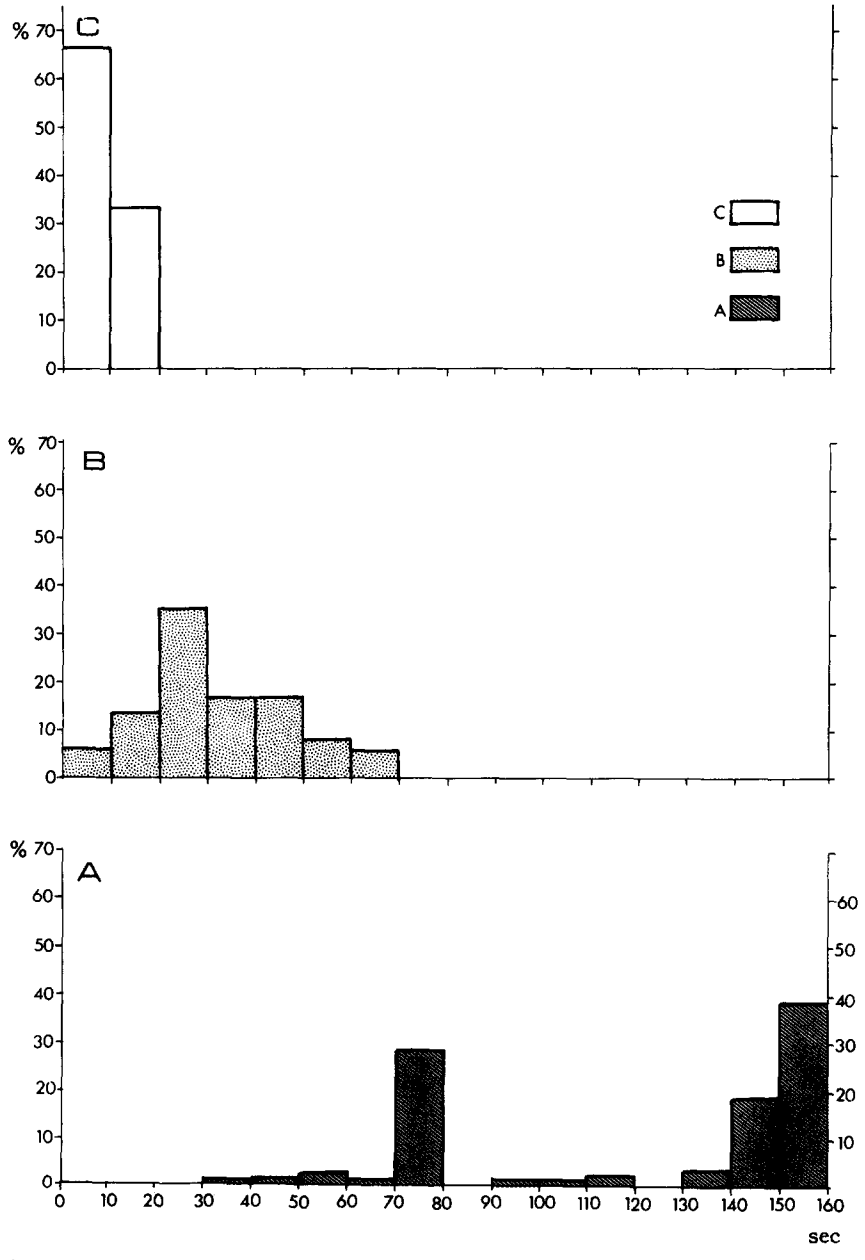

Fig. 13. Peak period features and distribution within the energy modes during the entire study period. (A) Infragravity. (B) Subharmonic. (C) Incident. Note two peaks in the infragravity range.

(Fig. 12). The shelter effect at the lee of an oblique bar contributes towards stability of the longshore flow direction in channelized feeders. Exposure to incident waves triggers directional fluctuations.

Spectra characteristics

The energy spectra of the total longshore currents, including currents and waves, showed a multimodal structure (Table 1). The mean distribution within the energy modes is shown on Fig. 13. The data indicates concentration of most energy (48–67%) in the gravity range, which totals significantly less than in the onshore–offshore currents — 60–87% (Bowman et al., 1988b).

Subharmonic energy composes 19–35%, a very similar magnitude to that found in onshore–offshore currents. Subharmonic edgewaves have been consistently reported for rip embayments (Huntley and Bowen, 1975; Guza and Inman, 1975; Wright et al., 1979). For gently sloping beaches their abundance was similar to our findings and much lower than of the incident waves (Huntley and Bowen, 1973).

The infragravity band contributes only minor energy (13–16%), however still double when compared to that band in shore normal currents (Bowman et al., 1988b). Dominant low-frequency spectral peaks of longshore currents have been reported by Woods and Meadows (1975), Guza and Thornton (1978), Holman et al. (1978) and

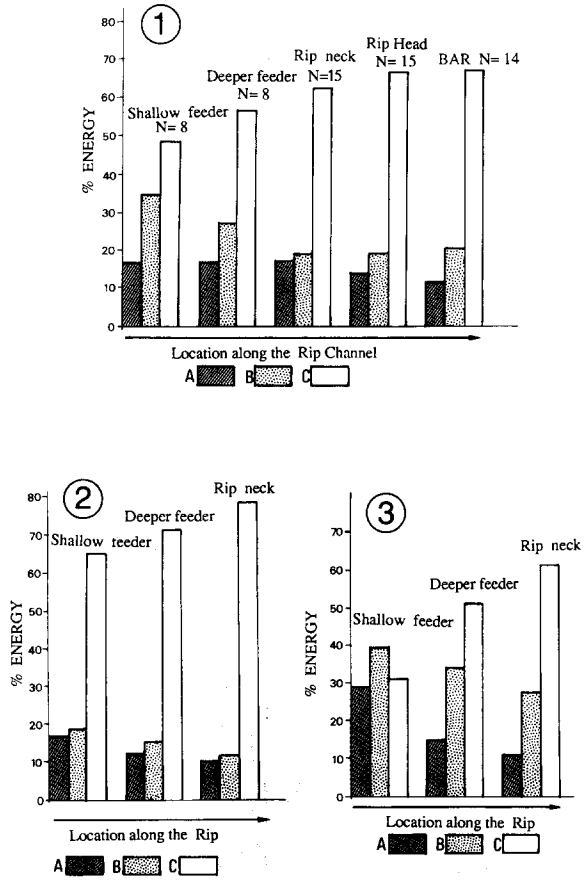

Fig. 14. Spatial trends of the longshore current energy spectra components in the rip system: A = infragravity, B = subharmonic, C = incident. (1) For the entire study period, and for 2 specific days: (2) 21/4/1983, (3) 6/9/1983.

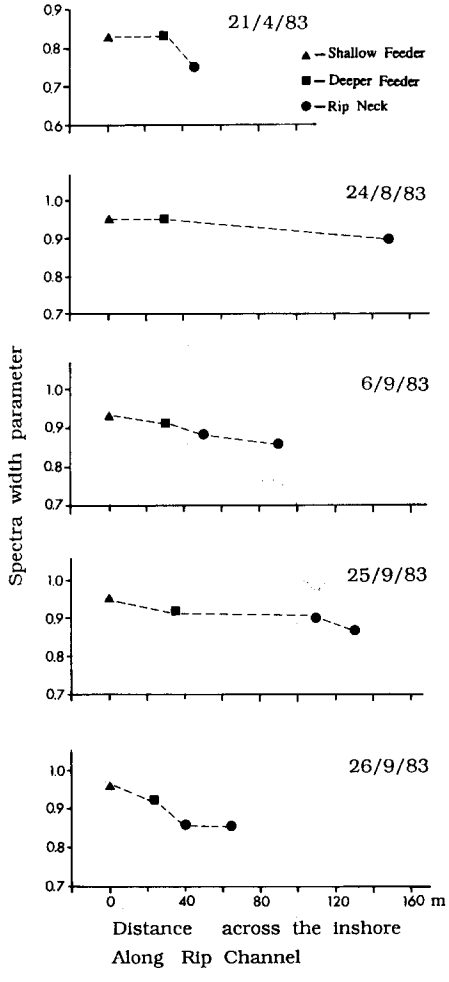

Fig. 15. Gradual narrowing of the spectra width toward the rip neck.

by others, and appear to be related to modes of edgewave phenomena.

Spatial trends of the spectra energy components along the rip system (Fig. 14) demonstrate a systematic intensification of the incident energy (C) towards the rip neck and head reflecting the gradual exposure to incident wave energy. Subharmonic energy of the longshore component across the rip system (B) demonstrates a complementary inverse trend, i.e., a gradual decay from the sheltered inshore towards the rip head. The infragravity energy component (A) is quite stable along the rip system, with a minor decay towards the offshore.

The overall dissipative to transitional state of our beaches seems to explain the relatively limited subharmonic band and the minor infragravity domain.

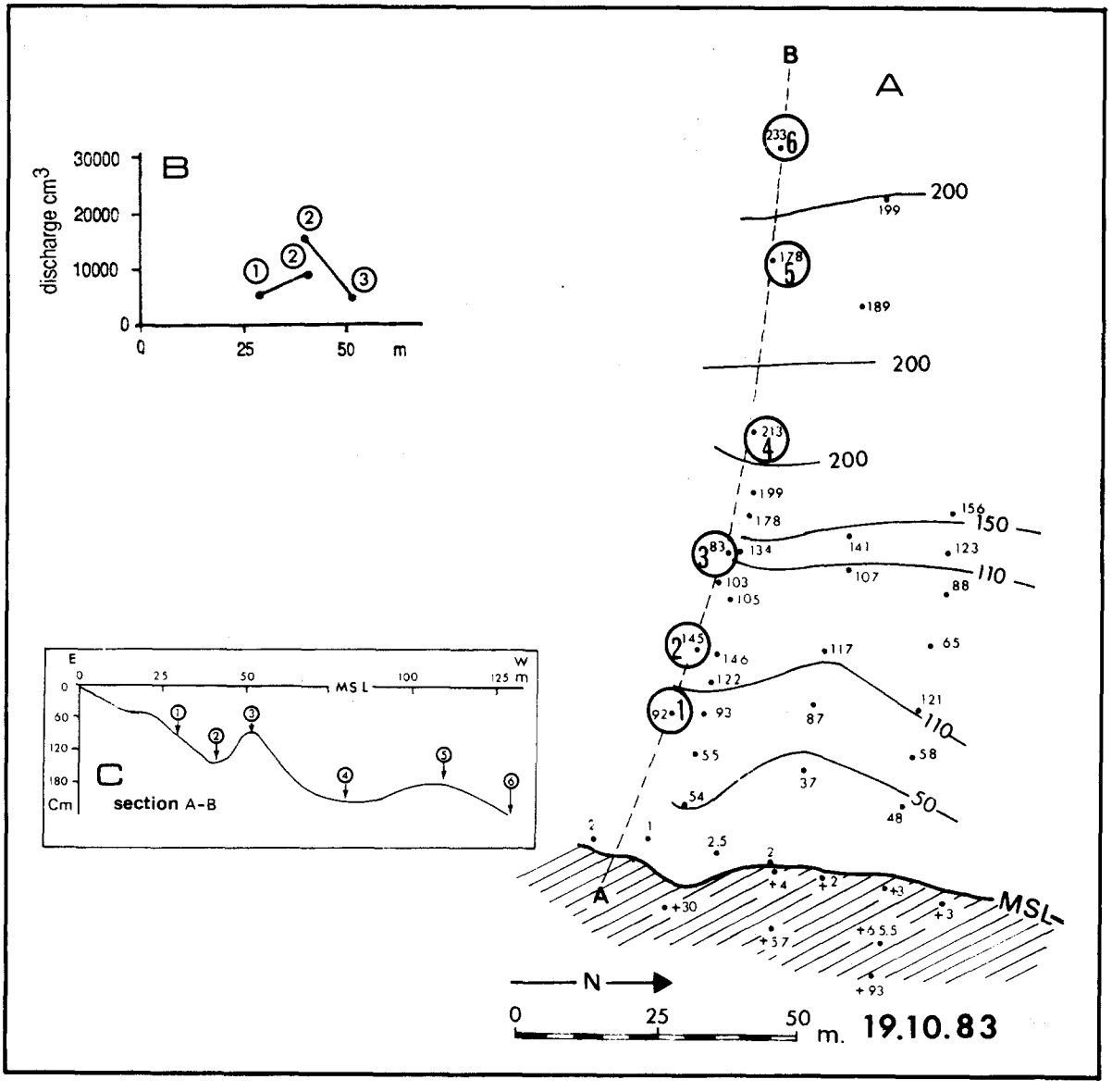

Fig. 16. Shore-parallel bar pattern. (A) Bathymetric map, depths in centimeters. Recording sites are encircled. (B) Net longshore velocity shown as discharge. (C) Bathymetric cross-section.

The spectra width parameter is a density index which shows the degree of the spectra peakedness. In oblique bar patterns the spatial trend shows decrease in the spectral width towards the rip neck (Fig. 15), which seems to reflect the gradual increase of the incident wave energy.

Summary

Although longshore current velocities are typically low (Shore Protection Manual, 1984), i.e., on or below threshold velocities for initiating motion of medium sand, the total longshore velocity, including waves and currents and the peak net longshore currents in low energy wave conditions, are very often in excess of the critical velocity.

The spectra demonstrates a characteristic energy structure. Incident wave energy made the primary contribution toward the longshore current. A clear shoreward gradual decay of the incident energy component accompanied by a gradual shoreward growth of the infragravity energy, stand out as main trends. The subordination of the infragravity signature demonstrates the overall transitional beach-state character. Furthermore, the relative abundance of subharmonic current energy is suggested as a distinguishing characteristic of the specific feeder subenvironment, probably highlighting its reflective character, of which such energy composition is the fingerprint (Wright and Short, 1984; Wright et al., 1986). In this respect the rip neck and head show a different energetic structure.

Our data indicate that high longshore velocity in rips occurs by the shoreline, seawards of the run-up. The feeder or neck are the sites of the fastest cross-rip longshore flow. The rip head is typified by the weakest longshore current. Here in calm weather the net longshore flow even drops below threshold velocity for sediment movement.

Nearshore bar patterns gain decisive control on the longshore flow through sheltering or exposing effects. In oblique bar systems with well-protected channels (Fig. 8, station 1), the ratio — maximum orbital velocity/maximum net longshore velocity — is minimized to 0.35–0.42. In a parallel bar

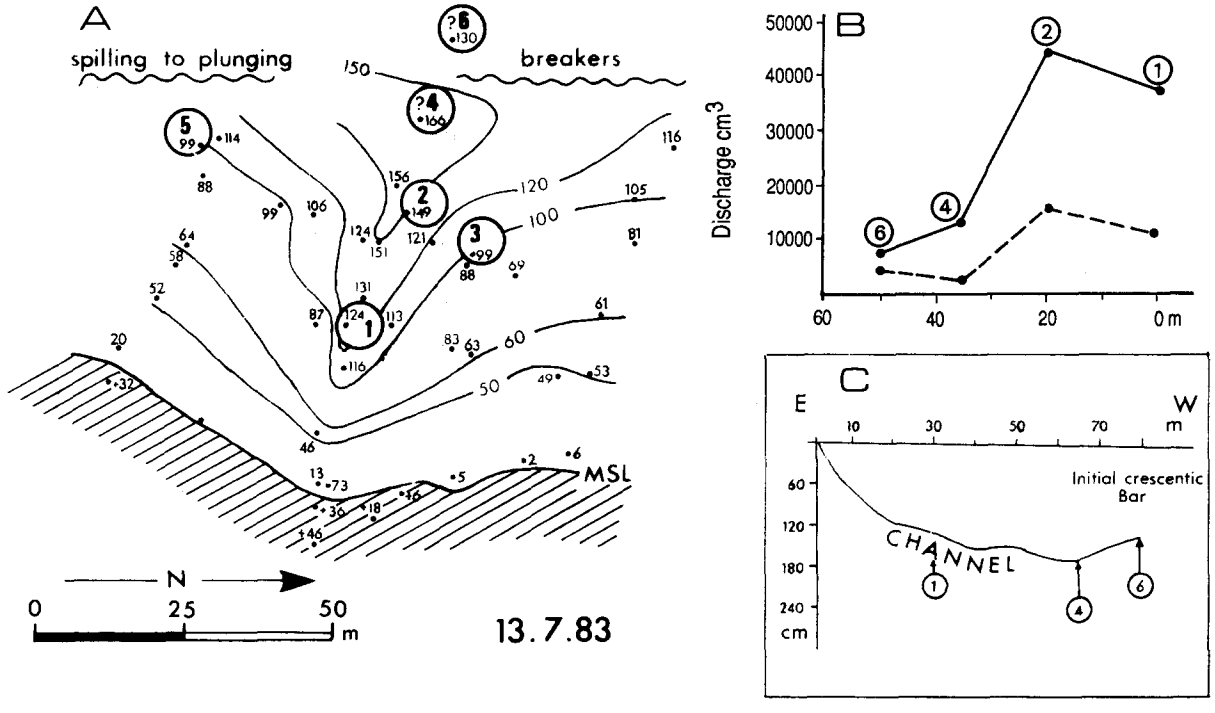

Fig. 17. Normal rip and bars. (A) Bathymetric map, depths in centimeters. Recording sites are encircled. (B) Net longshore velocity shown as discharge. Rip flow along the channel is shown as a broken line. (C) Bathymetric cross-section.

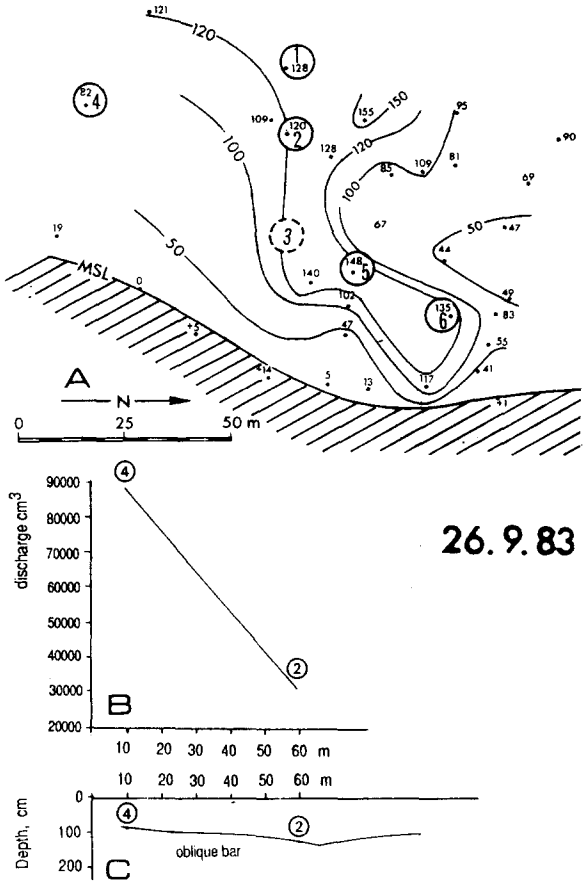

Fig. 18. Oblique rip and bars. (A) Bathymetric map, depths in centimeters. Recording sites are encircled. (B) Net longshore velocity shown as discharge. (C) Bathymetric cross-section.

system, when rips do not exist, the velocities of longshore currents are highest in the shore parallel channel (Fig. 16, station 2), whereas on the flanking bars and slope (stations 1 and 3) slower longshore currents were recorded, probably because of exposure to incident wave-induced oscillations. Similar results were reported by Greenwood and Sherman (1983) and by Davidson-Arnott and McDonald (1989). In a transverse bar system, because of higher exposure (Fig. 17, station 1), the orbital/longshore velocity ratio does not fall below 0.6–0.88. Here, the rip flow is continuously dominant and the longshore current is at minimum (Fig. 17B). After crossing the rip channel, the longshore current is intensified towards the bars (Fig. 18, station 4), because of the hydraulic shallowing effect.

Acknowledgement

This study was fully supported by the Earth Science Research Administration of the Ministry of Energy and Infrastructure. The help of Professor Ben Yaaqov of the Department of Electrical & Computer Engineering, Ben-Gurion University of the Negev, is highly appreciated. Thanks also to Mrs. Sharona Lazar and Pieter Louppen for the drafting work and to Mrs. Eunice Harrington for the typing.

References

Allen, P.A., 1985. Hummocky cross stratification is not produced purely under progressive gravity waves. Nature, 313: 562–564.

Allender, J.H. and Ditmars, J.D., 1981. Field Measurements of Longshore currents on a barred beach. Coast. Eng., 5: 295–309.

Arthur, R.S., 1962. A note on the dynamics of rip currents. J. Geophys. Res., 67: 2777–2779.

Basco, D.R., 1982. Surf zone currents—state of knowledge. Coastal Eng. Res. Cen. Misc. Rep., 82-7 I, 243 pp.

Basco, D.R., 1983. Surf zone currents. Coastal Eng., 7: 331–355.

Birkemeier, W.A. and Dalrymple, R.A., 1975. Nearshore water circulation induced by wind and waves. Proc. Symp. on Modelling Technique. Am. Soc. Civ. Eng., New York, pp. 1062–1081.

Bowen, A.J., 1969. Rip currents. 1. Theoretical investigations. J. Geophys. Res., 74: 5467–5478.

Bowen, A.J. and Inman, D.L., 1969. Rip currents, 2. Laboratory and field investigations. J. Geophys. Res., 74: 5479–5490.

Bowman, D., Rosen, D.S., Kit, E., Arad, D. and Slavicz, A., 1988a. Flow characteristics at the rip current neck under low energy conditions. Mar. Geol., 79: 41–54.

Bowman, D., Arad, D., Rosen, D.S., Kit, E., Goldbery, R. and Slavicz, A., 1988b. Flow characteristics along the rip current system under low energy conditions. Mar. Geol., 82: 149–167.

Carmel, Z., Inman, D.L. and Golik, A., 1984. Transport of Nile sand along the southwestern Mediterranean. Proc. 19th Coast. Eng. Conf. ASCE, pp. 1282–1290.

Clifton, H.E., 1976. Wave formed sedimentary structures, a conceptual model. SEPM Spec. Publ., 24: 126–148.

Cook, D.O., 1970. The occurrence and geologic work of rip currents off Southern California. Mar. Geol., 9: 173–186.

Cunningham, P.M., Guza, R.J. and Lowe, R.L., 1979. Dynamic Calibration of electromagnetic flow meters. Inst. Electron. Eng., Oceans, 79: 298–301.

Davidson-Arnott, R.G.D. and Greenwood, B., 1974. Bedforms and structures associated with bar topography in the shallow water environment. Kouchibouguac Bay, New Brunswick, Canada. J. Sediment. Petrol., 44: 698–704.

Davidson-Arnott, R.G.D. and Greenwood, B., 1976. Facies

relationships on a barred coast. Kouchibouguac Bay, New Brunswick, Canada. In: R.A. Davis and R.L. Ethington (Editors), Beach and Nearshore Sedimentation. SEPM Spec. Publ., 24: 140–168.

Davidson-Arnott, R.G.D. and McDonald, A., 1989. Nearshore water motion and mean flow in a multiple parallel bar system. Mar. Geol., 86: 321–338.

Dean, R.G., 1973. Heuristic Models of Sand Transport in the Surf Zone. Sydney, N.S.W., 239 pp.

Dingler, J.R. and Inman, D.L., 1977. Wave-formed ripples in nearshore sands. Proc. 15th Coast. Eng. Conf. ASCE, pp. 2109–2126.

Draper, L. and Dobson, P.J., 1965. Rip currents on a Cornish beach. Nature, 20: 1249.

Greenwood, B. and Davidson-Arnott, R.G.D., 1979. Sedimentation and equilibrium in wave formed bars: A review and case study. Can. J. Earth. Sci., 16: 312–332.

Greenwood, B. and Hale, P.B., 1980. Depth of activity, sediment flux and morphological change in the barred nearshore environment. In: S.B. McCann (Editor), The Coastline of Canada. Geol. Surv. Can., 80(10): 89–109.

Greenwood, B. and Sherman, D.J., 1983. Shore-parallel flows in a barred surf zone. Proc. 18th Coastal Eng. Conf. ASCE, pp. 1677–1696.

Goldsmith, V. and Golik, A., 1980. Sediment transport model of the Southeastern Mediterranean Coast. Mar. Geol., 37: 147–175.

Guza, R.T. and Inman, D.L., 1975. Edge waves and beach cusps. J. Geophys. Res., 80: 2997–3012.

Guza, R.T. and Thornton, E.B., 1978. Variability of longshore currents. Proc. 16th Coast. Eng. Conf. ASCE, 755–774.

Guza, R.T. and Thornton, E.B., 1980. Local and shoaled comparisons of sea surface elevations, pressures and velocities. J. Geophys. Res., 85: 1524–1530.

Holman, R.A., Huntley, D.A. and Bowen, A.J. 1978. Infragravity waves in storm conditions. Proc. 16th Coast. Eng. Conf. ASCE, pp. 268–284.

Huntley, D.A. and Bowen, A.J., 1973. Field observations of edge waves. Nature, 243: 160–162.

Huntley, D.A. and Bowen, A.J., 1975. Field observations of edge waves and their effect on beach material. J. Geol. Soc. London, 131: 69–81.

Huntley, D.A., Hendry, M.D., Haines, J. and Greenidge, B., 1988. Waves and Rip Currents on a Caribbean Pocket Beach, Jamaica. J. Coastal Res., 4: 69–79.

Inman, D.L. and Quinn, W.H., 1952. Currents in the surf zone. Proc. 2nd Coast. Eng. Conf., ASCE pp. 24–26.

Keeley, J.R. and Bowen, A.J., 1977. Longshore variations in longshore currents. Can. J. Earth. Sci., 14: 1897–1905.

Kit, E., Rosen, D.S., Slavicz, A. and Bowman, D., 1985. Analysis of Current Data. Coastal Mar. Eng. Res. Inst., Technion City, Haifa, P.N. 145/85, 684 pp.

Komar, P.D., 1976. Beach processes and sedimentation. Prentice Hall, Englewood Cliffs, N.J., 429 pp.

Lenhart, R.J., 1979. Nearshore marine bedforms, formative processes, distribution and internal structures. Ph.D. Thesis, Univ. Cincinnati, 166 pp.

Longuet-Higgins, M.S., 1970. Longshore currents generated by oblique incident sea waves. J. Geophys. Res., 75: 6778–6801.

Longuet-Higgins, M.S. and Stewart, R.W., 1964. Radiation stress in water waves: A physical discussion with application. Deep-Sea Res., 114: 529–562.

Meadows, G.A., 1977. Time-dependent fluctuations in longshore currents. Proc. 15th Coast. Eng. Conf. ASCE, pp. 660–680.

Migniot, C., 1974. Creation of a nuclear power station north of Hadra—Natural phenomena study. Lab. Cent. Hydr. Fr. Rep. for Isr. Electr. Co., 34 pp.

Neev, D. and Emery, K.O., 1967. The Dead Sea: depositional processes and environments of evaporates, Israel. Isr. Geol. Surv. Bull., 41, 147 pp.

Noda, E.K., 1974. Wave-induced nearshore circulation. J. Geophys. Res., 79: 4097–4106.

Rosen, D.S. and Kit, E., 1981. Evaluation of the wave characteristics at the Mediterranean coast of Israel. Isr. J. Earth Sci., 30: 120–134.

Rosen, D.S. and Vajda, M., 1979. Hadera wind and wave climate. Coastal Mar. Eng. Res., Inst., Technion City, Haifa, Israel, P.N. 47/79, 7 pp.

Sasaki, T. and Horikawa, K., 1975. Nearshore current system on a gently sloping bottom. Coastal Eng. Jpn., 18: 123–142.

Sasaki, T. and Horikawa, K., 1978. Observation of nearshore current and edge waves. Proc. 15th Coast. Eng. Conf. ASCE, pp. 791–809.

Shepard, F.P. and Inman, D.L., 1950. Nearshore circulation related to bottom topography and wave refraction. Eos., Trans. Am. Geophys. Union, 31: 555–565.

Short, A.D., 1985. Rip current type, spacing and persistence, Narrabeen beach, Australia. Mar. Geol., 65: 47–71.

Sonu, C.J., 1972. Field observation of nearshore circulation and meandering currents. J. Geophys. Res., 77: 3232–3247.

Tam, C.K.W., 1973. Dynamics of rip currents. J. Geophys. Res., 78: 1937–1943.

Woods, W.L. and Meadows, G.A., 1975. Unsteadiness in longshore currents. Geophys. Res. Lett., 2(11): 503–505.

Wright, L.D., Chappell, J., Thom, B.G., Bradshaw, M.P. and Cowell, P., 1979. Morphodynamics of reflective and dissipative beach and inshore systems: Southeastern Australia. Mar. Geol., 32: 105–140.

Wright, L.D., 1982. Field observations of long period surf zone oscillations in relation to contrasting beach morphologies. Aust. J. Mar. Freshwater Res., 33: 181–201.

Wright, L.D. and Short, A.D., 1984. Morphodyhnamic variability of surf zones and beaches: a synthesis. Mar. Geol., 56: 93–118.

Wright, L.D., Nielsen, P., Shi, N.C. and List, J.H., 1986. Morphodynamics of a bar–trough surf zone. Mar. Geol., 70: 251–285.

Wu, C.S., and Liu, P.L.F., 1985. Finite element analysis of nonlinear nearshore currents. J. Waterway Port Coastal Ocean Div., Am. Soc., Civil Eng., 111(2): 417–432.